Water Environment Federation
the water quality people

The influence of wind in secondary settling tanks for wastewater treatment—A computational fluid dynamics study. Part I: Circular secondary settling tanks

Haiwen Gao, Michael K. Stenstrom*

Department of Civil and Environmental Engineering, University of California Los Angeles, Los Angeles, California

Received 15 April 2019; Revised 17 September 2019; Accepted 19 September 2019

Correspondence to: Michael K. Stenstrom, Department of Civil and Environmental Engineering, University of California Los Angeles, Los Angeles, CA.
Email: stenstro@seas.ucla.edu

*WEF Member/Fellow

Published online 24 October 2019 in Wiley Online Library (wileyonlinelibrary.com)

DOI: 10.1002/wer.1241

• Abstract

Computational fluid dynamics model is used to understand the impact of wind on the performance of a secondary settling tank (SST) in a wastewater treatment plant (WWTP). Unlike most of the previous modeling studies which evaluated the wind effect on the settling tank in a water treatment plant, this study evaluates a circular SST in a WWTP at different current velocities and flow conditions. Performance indicators, such as effluent suspended solids and sludge blanket height, and three-dimensional hydrodynamics profiles are compared among different windy conditions and the calm condition and under different wind directions and flow conditions. The simulation results show that the existence of wind has strong negative impacts on the overall performance of the circular SST. The prediction of ESS is doubled in the circular SST under the mild wind condition. Moreover, the circular SST is more sensitive to the wind along the inlet port direction. © 2019 Water Environment Federation

• Practitioner points

- This is the first comparison of wind effects on a circular secondary settling tank
- Detailed computational fluid dynamics solution procedures to simulate a secondary settling tank
- Wind effects are investigated under multiple flow conditions, current velocities, and wind directions
- The performance of a circular secondary settling tank is very sensitive to the wind
- Wind along the inlet port direction has stronger negative impacts than it along 45° to the inlet direction

• Key words

circular secondary settling tank; computational fluid dynamics; turbulent flow; wastewater treatment plant

Introduction

Secondary settling tanks (SSTs), also known as sedimentation tanks or secondary clarifiers, are used in wastewater treatment plants (WWTPs) to remove organic matter and reduce nutrients such as nitrogen and phosphorus (Ramin et al., 2014). It has two different functions: clarification and thickening (Parker, 1983). Clarification separates the suspended solids (SS) to produce a low TSS effluent, while thickening concentrates the solids at the tank bottom in order to recycle or dispose with less volume (Gao & Stenstrom, 2017).

McCorquodale, Motta, Griborio, Georgiou, and Homes (2004) summarized that the efficiency of the SSTs depends on several influential factors, including (a) tank geometry, (b) flow conditions (surface overflow rate (SOR), returned activated sludge (RAS) ratio, and concentration of mixed liquor suspended solids (MLSS), and (c) atmospheric conditions, such as water temperature and wind velocity.

In the last three decades, many researchers and engineers have developed and applied computational fluid dynamics (CFD) models to optimize SST internal geometry to improve process efficiency and to understand the effects of influential factors on the efficiency of SSTs (Das et al., 2016; De Clercq, 2003; Ekama et al., 1997; Patziger, 2016; Ramalingam et al., 2012; Samstag, Dittmar, Vitasovic, & McCorquodale, 1992; Vitasovic, Zhou, McCorquodale, & Lingren, 1997; Weiss, Plósz, Essemiani, & Meinhold, 2007; Zhou & McCorquodale, 1992a, 1992b, 1992c). Most of the previous researches focused on the influential factors inside the SST, such as tank geometry, energy dissipating inlet structures, other baffle configurations, and flow conditions. However, the effects of the atmospheric conditions, such as wind, have rarely been studied.

Larsen (1977) identified that the wind shear at the free surface transfers energy to the SST and affects the flow field. McCorquodale et al. (2004) noted the wind is one of the influential factors on the performance of an SST. However, their Q3D model did not include the wind shear effects because of limited computing resources, and they concluded that SST models should be expanded to three dimensional (3D) to accurately predict wind effects.

In the recent years, several researches have studied the wind effects on rectangular settling tanks in water treatment plants (WTPs) (Gkesouli, Nitsa, Stamou, Rutschmann, & Bui, 2016; Gkesouli & Stamou, 2018; Goodarzi, Lari, & Alighardashi, 2018; Khezri, Biati, & Erfani, 2012; Stamou & Gkesouli, 2015). Table 1 shows the major conclusions of these studies. In most cases, the predicted effects on removal efficiency are negative, with the exception of low counter-current wind velocity, which increased ESS removal. However, the applicability of these studies to SSTs in WWTPs is limited since the particle concentration in the influent of the settling tank in WTPs is very low. The effects of particles on the flow field are negligible, whereas the high particle concentration in the influent of SSTs in WWTPs makes the flow currents density-driven.

Additionally, settling tanks in WTPs are usually rectangular tanks, whereas circular tanks are often used in large SSTs in WWTPs. Also, the internal baffling structures for rectangular and circular settling tanks are different. Therefore, the flow and concentration fields for settling tanks in WTPs and SSTs in WWTPs are different, and results concluded for settling tanks in WTPs may not be appropriate for SSTs in WWTPs. To the best of our knowledge, none of the published papers simulated the wind effects on SSTs in WWTPs.

This study differs from the previous wind studies on settling tanks in WTPs in that high total suspended solids (TSS) concentrations, which causes density currents are considered. The circular SST in a WWTP is studied under different flow rates and wind directions and velocities. The geometry of SST and flow conditions is adapted from McCorquodale et al. (2004). Table 2 summarizes the loading conditions of the Darvill SST. The CFD package ANSYS Fluent v18.2 is used to simulate the wind effects on the circular SST along the inlet port direction (along *x*-axis) and at 45° to the inlet direction, and Tecplot 360 (Bellevue, WA) is used for postprocessing.

Ideally, a transient, 3D and three-phase SST model is needed to simulate an SST that take into account the effect of wind. However, a single run of such simulation may require a few months with our computer (Xeon Sliver 4114). Gkesouli and Stamou (2018) provided an alternative, but more economical and faster approach, which is to determine a typical value of the current velocity at the water surface (Us) and set it as a boundary condition along the water surface. The Us is expected to depend on the velocity of the wind that is usually defined at a height of 10 m (U_{10}) or "tree top" wind velocities.

Under each tested wind direction, the current velocity at the water surface (U_s) increases from zero to two mildly windy

Table 1. Summary of major contributions of previous studies on wind effects on rectangular water treatment plant settling tanks

REFERENCES	WIND SPEED (U_{10})/SURFACE FLOW SPEED (U_S)	MAJOR CONCLUSIONS
Khezri et al. (2012)	U_{10} = 2.5–7.0 m/s (both co-current and counter-current)	Co-current wind causes increase flow field velocity resulting in reduced particle removal efficiency Counter-current wind causes flow field velocity decrease that improve particle removal efficiency at low wind velocities (0–2.5 m/s), but reduced removal efficiency at high velocity (>2.5 m/s)
Stamou and Gkesouli (2015)	U_s = 0.5 m/s (co-current only)	Co-current wind causes negligible effects on particle removal efficiency
Gkesouli et al. (2016)	U_{10} = 0, 5, 7.5 m/s (both co-current and counter-current)	Co-current wind slightly reduces particle removal efficiency (<0.3%) Counter-current wind slightly increases particle removal efficiency by up to 1%
Goodarzi et al. (2018)	U_{10} = 5.0 m/s (co-current only)	Co-current wind causes strong negative effects on particle removal efficiency
Gkesouli and Stamou (2018)	U_{10} = 15–25 m/s (co-current only)	Co-current wind causes strong negative effects on removal efficiency

Table 2. Loading conditions of the Darvill SST

	INFLOW PARAMETERS			SETTLING PARAMETERS			DRY SOLIDS DENSITY
	MLSS	RAS	$Q_{EFFLUENT}$	V_O	R_H	R_P	P_P
TESTS NO.	G/L	RATIO	M^3/HR	M/HR	L/G	L/G	KG/M^3
Case 1	4.60	0.80	833	7.71	0.39	10.00	1,450
Case 2	4.30	0.97	688	7.71	0.39	10.00	1,450
Case 3	3.60	0.79	948	7.71	0.39	10.00	1,450

conditions (U_s = 0.125 and 0.25 m/s) and one extreme condition (U_s = 0.50 m/s), which correspond to 8.35, 16.69, and 33.39 miles/hr for the averaged wind velocities at 10 m height (U_{10}), respectively. Equation (1) shows the conversion between U_s and U_{10} (Gkesouli & Stamou, 2018). Table 3 shows the conversion between the U_s and the averaged U_{10}.

$$U_s = (0.9\% - 5.8\%)\, U_{10} \tag{1}$$

Performance indicators, such as effluent suspended solids (ESS), and sludge blanket height (SBH) from the tank surface, and 3D hydrodynamics profiles, are compared as in the range of different wind speeds and wind directions. The SBH is defined as the depth of sludge bed contour 1,000 mg/L to the water surface.

Methods

The mathematical model

General information. The hydrodynamics characteristics of settling tanks in WTPs were studied by using the standardized multiphase model based on a theoretical solution for slip velocity based on particle size (Gkesouli et al., 2016; Goodarzi et al., 2018; Stamou & Gkesouli, 2015). However, since the flow in SST is driven by density current, the particle transport model based on sludge settling velocities perform better than the standardized multiphase model (Wicklein & Samstag, 2009). Therefore, the particle transport model based on sludge settling velocities used in our previous SST studies (Gao & Stenstrom, 2018a, 2018b, 2019a, 2019b) is also coupled in this current study.

Governing equation. The equations describing 3-D, transient, turbulent, and density stratified flow in a circular SST are as follows (Das et al., 2016):

Continuity equation:

$$\frac{\partial \rho}{\partial t} + \nabla \cdot \left(\rho \vec{u_i}\right) = 0 \tag{2}$$

Momentum equation:

$$\frac{\partial \rho \vec{u_i}}{\partial t} + \nabla \cdot \left(\rho \vec{u_i}\vec{u_i}\right) = -\nabla p + \nabla \cdot \bar{\bar{\tau}} + \vec{F} \tag{3}$$

Standard k-ε turbulence model:

$$\frac{\partial \rho k}{\partial t} + \rho \nabla \left(\vec{u_i} k\right) = \rho \nabla \left[\left(\nu + \frac{\nu_t}{\sigma_k}\right) \nabla k\right] + G_k + G_b - \rho\varepsilon \tag{4}$$

$$\frac{\partial \rho \varepsilon}{\partial t} + \rho \nabla \left(\vec{u_i}\varepsilon\right) = \rho \nabla \left[\left(\nu + \frac{\nu_t}{\sigma_\varepsilon}\right) \nabla \varepsilon\right] + C_1 \frac{\varepsilon}{k}\left(G_k - C_3 G_b\right) - C_2 \rho \frac{\varepsilon^2}{k} \tag{5}$$

Sludge transport equation:

$$\frac{\partial \rho C}{\partial t} + \frac{\partial \rho \left(\vec{u_i} + V_s\right) C}{\partial x_i} = \rho \frac{\partial}{\partial x_i}\left[\left(\nu + \frac{\nu_t}{\sigma_c}\right) \frac{\partial C}{\partial x_i}\right] \tag{6}$$

Sludge settling equation (Takács, Patry, & Nolasco, 1991):

$$V_s = \max\left(0, V_o\left(e^{-r_p\left(C - C_{\min}\right)} - e^{-r_h\left(C - C_{\min}\right)}\right)\right) \tag{7}$$

Sludge rheological model (Bokil, 1972):

$$\nu = 1 \times 10^{-6} e^{1.386C} \text{ for } C \le 1 \text{ g/L} \tag{8}$$

and

$$\nu = 2.9 \times 10^{-6} e^{0.322C} \text{ for } C \ge 1 \text{ g/L}$$

Local fluid density:

$$\rho = \rho_r + C\left(1 - \frac{\rho_r}{\rho_p}\right) \tag{9}$$

where ρ is the local fluid density, t is time, $\vec{u_i}$ is the absolute velocity vector, p is the general pressure less the hydrostatic pressure at reference density ρ_r, $\bar{\bar{\tau}}$ is viscous stress, $\vec{F}$ is body force, and k in Equation (4) and ε in Equation (5) are turbulent kinetic energy (TKE) and turbulent dissipation rate, respectively. G_k represents the generation of TKE due to the mean velocity gradients, and G_b corresponds to the generation of TKE due to buoyancy. ϑ is the viscosity of the sludge mixture, and ϑ_t is the turbulent eddy viscosity. In Equation (6), C is the sludge concentration, V_s is the sludge settling velocity in the vertical direction, and σ_c is the

Table 3. Relationship between flow velocities on the water surface (U_s) and "tree top" wind velocities (U_{10})

U_S = (0.9%–5.8%) U_{10}			
U_s (m/s)	0.125	0.25	0.50
$U_{10\_Averaged}$ (m/s)	3.73	7.46	14.93
$U_{10\_Averaged}$ (miles/hr)	8.35	16.69	33.39

Note. $U_{10\_Averaged}$ (m/s) = U_s/3.35%.

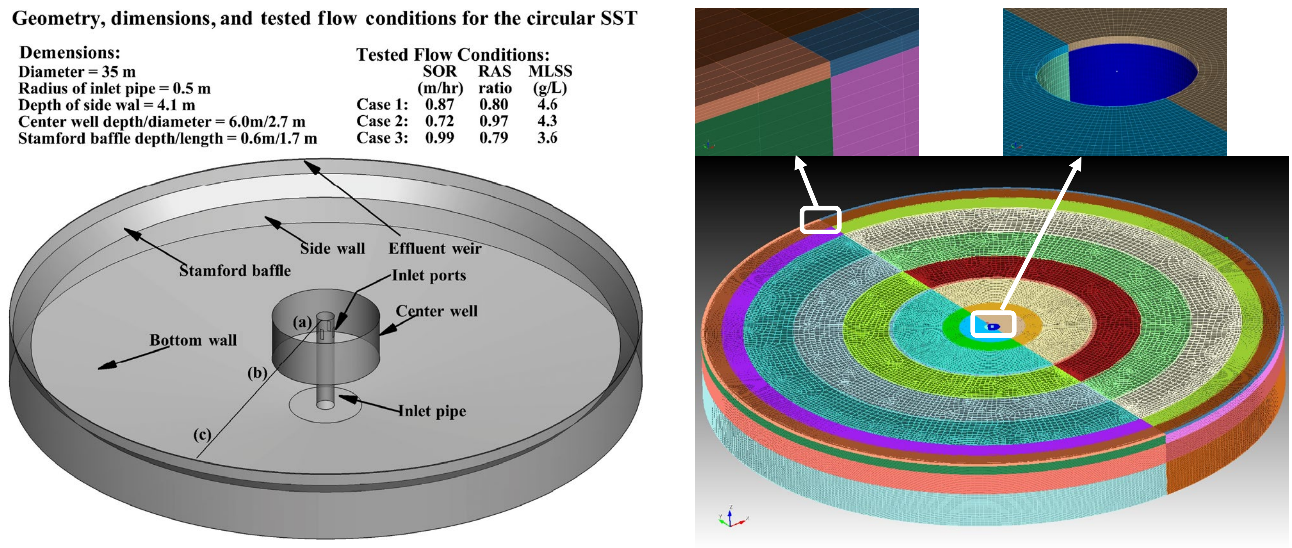

Figure 1. Geometry, dimensions, the tested flow conditions (left), and mesh (right) for the circular SST. (a–c) refer to the locations for grid independent tests shown in Figure 2.

turbulent Schmidt number. The value of σ_c is assumed to be 0.7 in this study (Lakehal et al., 1999). Gao and Stenstrom (2018b) studied its effects on the performance of SSTs and found that σ_c can be used to adjust the sludge blanket height (SBH), when effluent suspended solids (ESS) and returned activated sludge (RAS) concentration are well calibrated to the field data. r_p and r_h account for rapidly and poorly settling floc, respectively. They were calibrated in the original study of this circular SST (McCorquodale et al., 2004).

Computational fluid dynamic boundary conditions. Velocity inlet boundary conditions are applied to inlet and sludge bottom boundaries, which assume a uniform distribution of all the dependent variables at the boundary face. For the surface outlet, a pressure outlet boundary condition is applied. Using this type of boundary condition, all flow quantities at the outlets are extrapolated from the interior domain. For the calm condition, the free ambient water surface is treated as a free slip wall. For the windy conditions, a constant horizontal velocity is used on the free surface along the wind direction (Gkesouli & Stamou, 2018; Stamou & Gkesouli, 2015). The solid boundaries are specified as stationary walls with a no slip-shear condition.

Solution procedure. 1. Solve the steady-state flow field with pure water. Convergence is reached when normalized residuals are $<10^{-3}$;

2. Switch the solver from steady to transient;
3. Coupled the solids transport equation defined in the user-defined scalar;
4. Change the pure water density to the user-defined fluid density;
5. Change the pure water viscosity to the user-defined fluid viscosity;

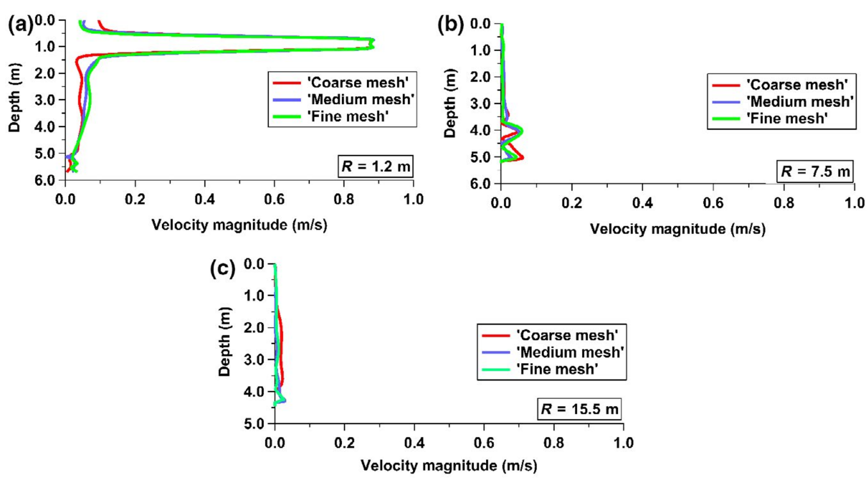

Figure 2. Grid independence test for calculated velocity magnitude (m/s) at three representative radial locations of the circular SST.

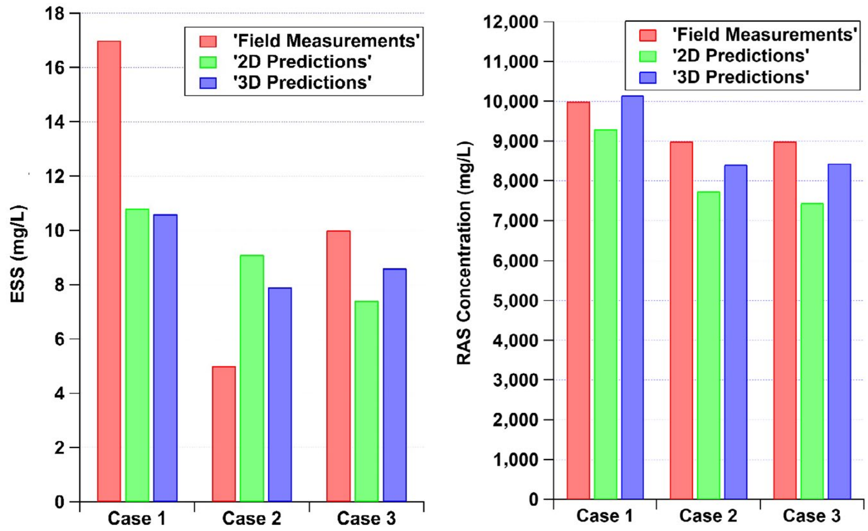

Figure 3. Comparisons among the predictions of performance indicators with 2D, 3D models, and field data.

6. The buoyancy damping term (G_b) is included to the TKE equation to describe the turbulent and density stratified flow;
7. Enable a surface monitor for the concentration of solids on surface outlet boundary;
8. Enable a surface monitor for the concentration of solids on sludge bottom boundary; and
9. Enable a volume monitor for the solids volume in the SST.

In the steps (2) to (9), convergence is achieved when the following three criteria are all achieved:

1. Normalized residuals are $<10^{-3}$ or the solution no longer changes with subsequent iterations;
2. The net flux imbalance is <1% of the smallest flux through the domain boundary; and
3. Other monitored key physical quantities no longer change with subsequent iterations.

Geometry and meshing

Figure 1 shows the geometries, dimensions, the tested flow conditions, and meshes for the circular SST. The computational mesh is generated from Trelis 16.5 (American Fork, Utah) and consists of a total number of 4.8 million hybrid cells. The geometry of the circular SST was cut axisymmetrically and automatically shown with different colors. Next, the geometry with half SST was cut into different sections along the radial direction and meshed in each section independently. The sections with different colors along the radial direction represent the mesh in different sizes, with finer meshes in the field near the inlet and outlets and coarser meshes in the main settling zone. Finally, the mesh for half of the geometry was duplicated to automatically generate the mesh for another half of the geometry. It should be noted that there are four inlet ports at the very center of the SST, and the direction of these ports is significant as shown in the simulations.

In order to ensure that the solutions are mesh independent, one coarser mesh consisting of 2.5 million cells and a finer one consisting of 8 million cells are used for the circular tank. Figure 2 shows velocity magnitudes as a function of depth for the circular SST calculated from meshes with different grid numbers at three positions along the radius on the downwind side of the SST. The three positions are shown in Figure 1 as (a–c). Since the prediction difference using the medium and fine meshes is negligible, solution from the mesh of 4.8 million cells for the circular SST is considered mesh independent and has the benefit of increased computational speed.

Model validation

The predictions of ESS and RAS are compared with the measured results (McCorquodale et al., 2004) and previous two-dimensional (2D) simulation results shown in our previous study (Gao & Stenstrom, 2018a). Figure 3 shows that predictions of the current 3D model are consistent with the previous 2D results and measured results. The case numbers in Figure 3 are listed in Figure 1.

Results and Discussion

Performance indicators

Figure 4 shows comparisons of predictions of area-weighted performance indicators among different current velocities at the water surface for Cases 1–3. It shows that the wind deteriorates the SST clarification performance, whereas it has little impact on sludge thickening until under the extreme windy condition. Also, wind along the inlet port direction has a stronger impact than a 45° to the inlet direction.

The SST clarification is very sensitive to the wind, especially when the concentration of MLSS is high. The prediction of ESS is approximately doubled as the increase in the current velocity at the water surface (U_S) to 0.125 m/s (U_{10} = 8.35 miles/hr) in each case. As the increase in the current velocity at the water surface (U_S) to 0.25 m/s (U_{10} = 16.69 miles/hr), the SST

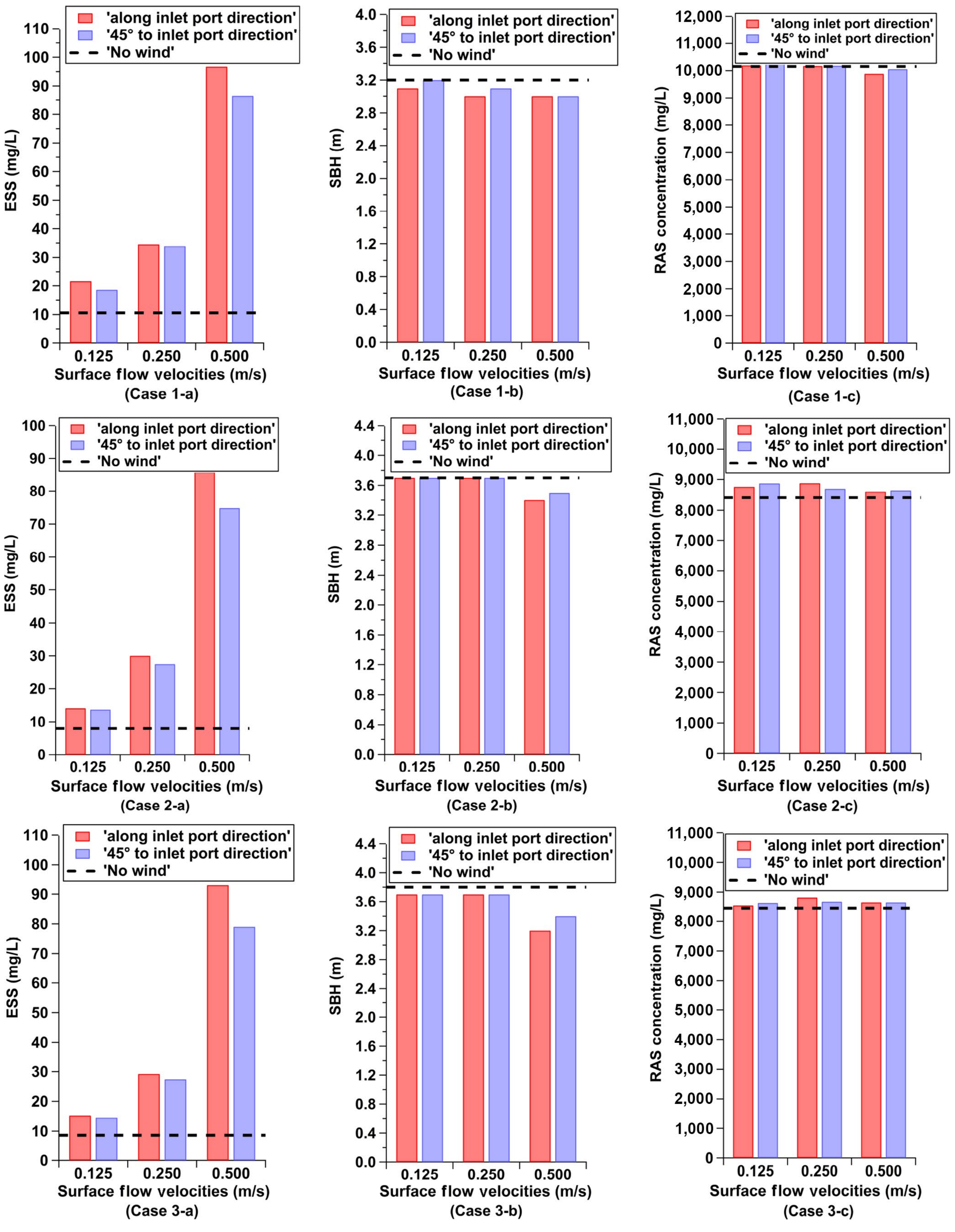

Figure 4. Predictions of area-weighted performance indicators among different flow velocities on the water surface for Cases 1–3. (Top: Case 1; Medium: Case 2; Bottom: Case 3).

Table 4. Predictions of performance indicators range among different flow velocities on the water surface for Cases 1–3

SURFACE FLOW SPEEDS	WIND DIRECTIONS	AVERAGED ESS (MG/L)	LOWEST ESS (MG/L)	HIGHEST ESS (MG/L)	AVERAGED RAS (MG/L)	AVERAGED SBH (M)
Case 1						
$U_s = 0$		10.6	5.4	27.0	10,151	3.2
$U_s = 0.125$ m/s	A	21.6	9.6	67.0	10,191	3.1
$U_s = 0.125$ m/s	B	18.6	10.0	44.0	10,262	3.2
$U_s = 0.25$ m/s	A	34.5	17.8	80.0	10,170	3.0
$U_s = 0.25$ m/s	B	33.9	17.9	78.3	10,180	3.1
$U_s = 0.50$ m/s	A	96.7	43.3	208	9,885	3.0
$U_s = 0.50$ m/s	B	86.4	41.0	167	10,056	3.0
Case 2						
$U_s = 0$		7.9	5.7	11.3	8,410	3.7
$U_s = 0.125$ m/s	A	14.1	9.0	25.0	8,756	3.7
$U_s = 0.125$ m/s	B	13.7	8.7	23.0	8,870	3.7
$U_s = 0.25$ m/s	A	30.0	17.5	55.0	8,876	3.7
$U_s = 0.25$ m/s	B	27.5	16.3	55.8	8,691	3.7
$U_s = 0.50$ m/s	A	85.8	38.3	196	8,600	3.4
$U_s = 0.50$ m/s	B	74.8	35.9	177	8,640	3.5
Case 3						
$U_s = 0$		8.6	3.0	14.0	8,440	3.8
$U_s = 0.125$ m/s	A	15.2	9.0	25.8	8,532	3.7
$U_s = 0.125$ m/s	B	14.5	9.0	23.4	8,633	3.7
$U_s = 0.25$ m/s	A	29.2	16.8	81.3	8,815	3.7
$U_s = 0.25$ m/s	B	27.4	16.6	51.6	8,674	3.7
$U_s = 0.50$ m/s	A	93.0	43.8	173	8,652	3.2
$U_s = 0.50$ m/s	B	79.0	39.0	162	8,652	3.4

Note. Wind directions: A: Along the inlet port direction; B: 45° to the inlet port direction.

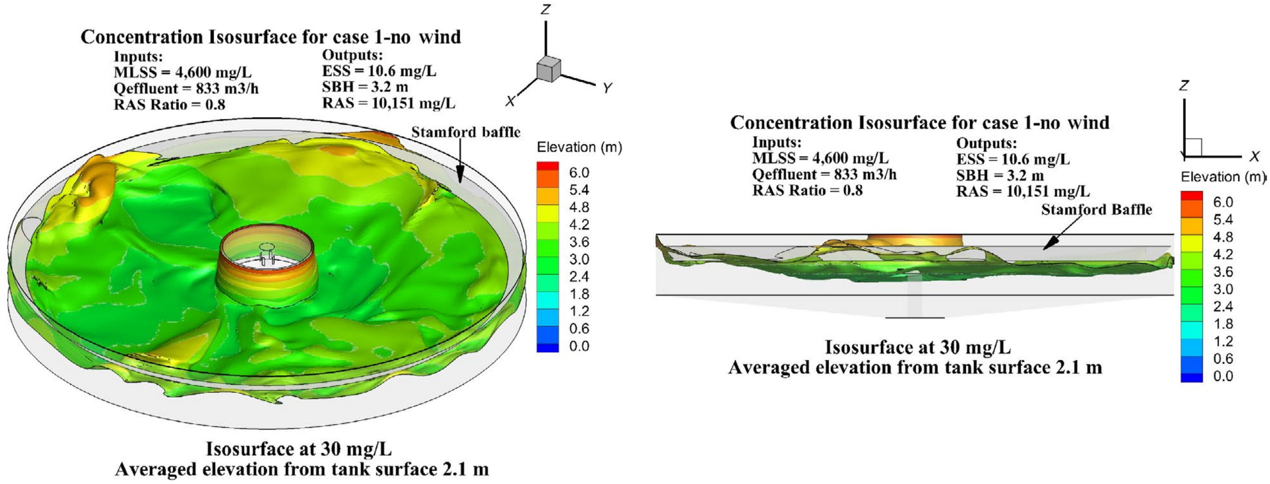

Figure 5. Concentration isosurface at 30 mg/L under the calm condition for the Case 1. Note the four inlet ports in the very center of the SST.

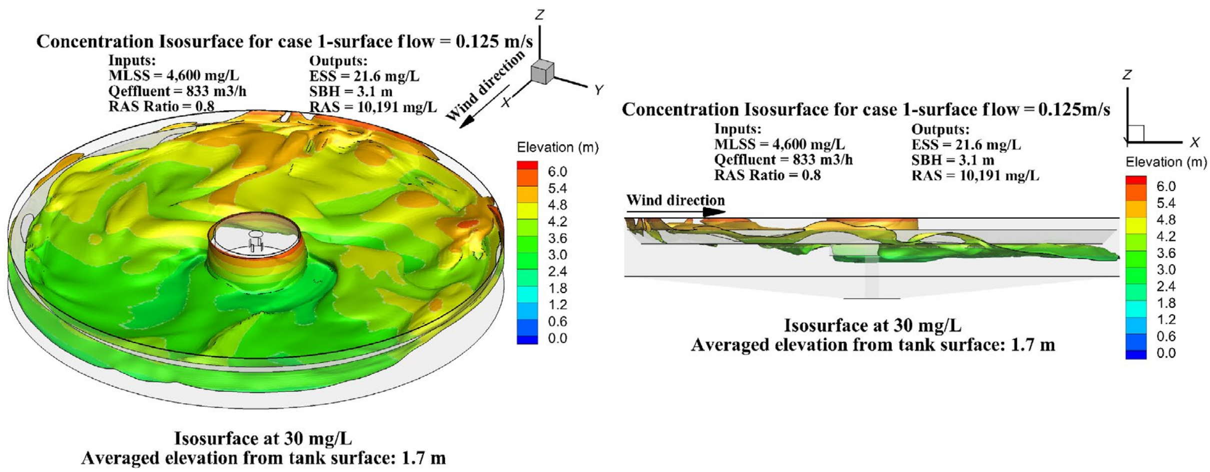

Figure 6. Concentration isosurface at 30 mg/L under the first windy condition (U_s = 0.125 m/s) for the Case 1.

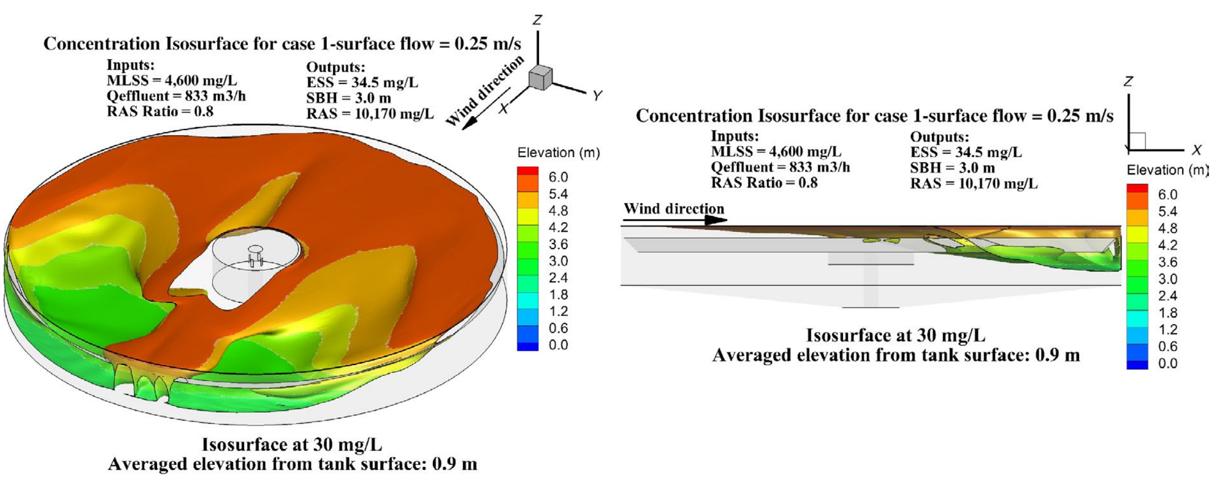

Figure 7. Concentration isosurface at 30 mg/L under the second windy condition (U_s = 0.25 m/s) for the Case 1.

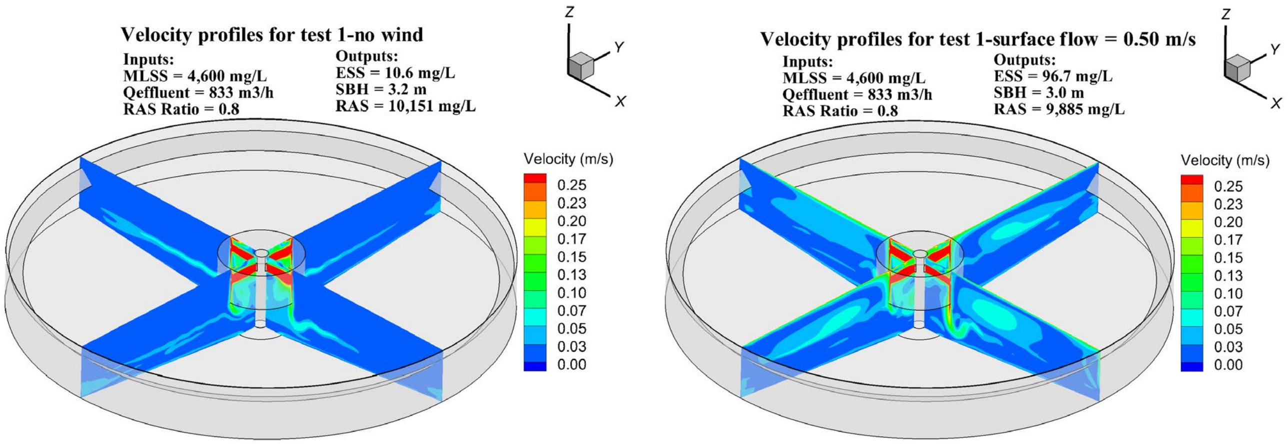

Figure 8. Velocity profiles without (left) and with (right) the wind effect.

fails in Case 1 due to the excessive of ESS and is under the limiting condition in both Cases 2 and 3.

Since the effects of turbulence and wind, the flow and concentration distribution are not uniform in the SST; therefore, the distribution of ESS is not uniform. Table 4 shows the predictions of performance indicators range among different current velocities at the water surface (U_S) for Cases 1–3. Although Figure 4 shows that the area-weighted ESS in Case 1 under the calm and mild windy condition (Us = 0.125 m/s) are much lower than the ESS limit (30 mg/L), Table 4 shows that the ESS is close to the limit in Case 1 under the calm condition and exceeds the ESS limit (highlighted in red) under the mild windy condition (Us = 0.125 m/s) at a certain location. Table 4 also indicates that the wind along the inlet port direction has a stronger impact on the SST clarification.

Concentration isosurfaces

In order to better illustrate the prediction results shown in Table 4, sludge concentration isosurfaces at 30 mg/L under calm and the first two windy conditions for the Case 1 are shown in Figures 5–7, respectively. Table 4 and Figure 4 show that the ESS exceeds 30 mg/L on the entire effluent weir under the extreme windy condition; therefore, the concentration isosurface at 30 mg/L under the extreme windy condition does not exist and cannot be shown here.

Figure 5 shows that due to the high concentration of MLSS, the 30 mg/L isosurface is generally close to the Stamford baffle. At some peripheral areas of the SST, the isosurface is above the Stamford baffle and is very close to the effluent weir. Therefore, the predicted ESS is close to 30 mg/L at these areas. Figure 6 shows that under the first mild windy condition (Us = 0.125 m/s), the elevation of the isosurface on the entire upwind side of the SST rises above the Stamford baffle. At some peripheral areas of the SST, the isosurface is at the effluent weir. Therefore, the SST clarification partially fails. Figure 7 shows that as the increase in the wind shear induced current velocity at the water surface (U_S = 0.25 m/s), the 30 mg/L isosurface on the entire upwind side of the SST is at the water surface. Also, the current velocity at the water surface (U_S) caused by the wind shear drifts the SS on the upwind side of the SST to the downwind side of the SST. Therefore, the SST clarification on the entire effluent weir fails.

Velocity profiles without/with the wind effect

Figure 8a,b shows the velocity profiles without/with the wind effect, respectively. Without the wind effect (left), inflows on both sides of the SST impinge on the center well and are then forced downward before reversing directions to form horizontal jets toward the side wall. In a vertical section of the SST, the horizontal jet in the main settling zone recirculates the flow clockwise and counterclockwise on both sides of the SST.

The existence of the wind (right) increases the circulation on the upwind side of the SST and causes a large and strong recirculation in the main settling zone. The horizontal jet flows along the radial direction to the side wall where it turns vertically and then turns back toward the center well. Therefore, the liquid in main settling zone of the upwind side of the SST is mixed, reducing clarification efficiency.

On the downwind side of the SST, the current velocity at the water surface caused by the wind effect creates opposite recirculation flows compared with the upwind side. The recirculation flow is along the surface, to the side wall then downward and back along the SST bottom to the center well. The wind flows against the horizontal flow to the center well. Therefore, the horizontal jet becomes weaker and the recirculation magnitude in the main settling zone is reduced compared with the upwind side. Also, the SS on the upwind side of the SST can be transported to the downwind side by the strong surface jet, the overall ESS removal efficiency of the SST decreases.

Conclusions

In this study, Fluent-based 3D transient model is used to analyze the impact of wind on the performance of a circular SST in an WWTP. The wind with three different speeds and two wind directions (along the inlet port direction and at 45° to the inlet port direction) are studied under three different flow conditions (Cases 1–3). Therefore, 21 simulations are run for the circular SST.

The predictions of performance indicators such as ESS and SBH and 3D hydrodynamics profiles are compared among different wind velocities and the calm condition. Additionally, predictions under different wind directions are also compared.

For the cases studied under various flow conditions, wind velocities, and wind directions, the following predictions and conclusions are made:

- The circular SST clarification performance is very sensitive to the wind. Wind deteriorates the SST clarification performance under every wind direction in the circular SST. The existence of the first mild windy condition ($U_s = 0.125$m/s) doubles the ESS for the circular SST (e.g., ESS increases from 10.8 to 22 mg/L for the Case 1) and existence of the second mild windy condition ($U_s = 0.25$m/s) causes the failure of the circular SST (e.g., ESS increases from 10.8 to 34 mg/L for the Case 1).
- For the circular SST, wind along the inlet port direction has stronger negative impact on the SST than the wind at 45° to the inlet direction. Also, as the increase in the wind speed, the discrepancy of the predicted ESS between these two wind directions increases.
- Under mild windy conditions ($U_s \leq 0.25$ m/s) from all directions, the wind has little effect on the sludge thickening in the circular SST; high wind ($U_s = 0.50$ m/s) deteriorates the sludge thickening. The change in the SBH under mild wind conditions is <0.2 m, while the change in the SBH under the extreme windy condition is more than 0.6 m.
- These results suggest that in windy climates, covering circular SSTs or protecting them from strong winds may be justified.

Data availability statement

The three programs we used are commercially available and we have referenced them. The calibration data are from a previously published study (Krebs, Stamou, Garcia-Heras, & Rodi, 1996), which we have referenced and is available Web of Science and Google Scholar databases.

References

Bokil, S. D. (1972). *Effect of mechanical blending on the aerobic digestion of the waste activated sludge*, Ph.D. thesis. Ontario, Canada: Department of Civil and Engineering, University of Windsor.

Das, S., Bai, H., Wu, C., Kao, J.-H., Barney, B., Kidd, M., & Kuettel, M. (2016). Improving the performance of industrial clarifiers using three-dimensional computational fluid dynamics. *Engineering Applications of Computational Fluid Mechanics*, *10*(1), 130–144.

De Clercq, B. (2003). *Computational fluid dynamics of settling tanks: development of experiments and rheological, settling, and scraper submodels*. BIOMATH. Ghent, Belgium: University of Ghent.

Ekama, G. A., Bernard, J. L., Gunthert, F., Krebs, P., McCorquodale, J., Parker, D., & Wahlberg, E. (1997). *Secondary settling tanks: Theory, modelling, design and operation* (pp. 187–203). Richmond, UK: International Association on Water Quality.

Gao, H., & Stenstrom, M. K. (2017). *Computational fluid dynamics applied to secondary clarifier analysis*. In Proceeding of the 17th Annual World Environmental and Water Resources Congress, pp. 301–315. Sacramento, CA.

Gao, H., & Stenstrom, M. K. (2018a). Evaluation of three turbulence models in predicting of the hydrodynamics of a secondary sedimentation tank. *Water Research*, *143*, 445–456.

Gao, H., & Stenstrom, M. K. (2018b). Turbulence and interphase mass diffusion assumptions on the performance of secondary settling tanks. *Water Environment Research*, *91*(2), 101–110.

Gao, H., & Stenstrom, M. K. (2019a). Generalizing the effects of the baffling structures on the buoyancy-induced turbulence in secondary settling tanks with eleven different geometries using CFD models. *Chemical Engineering Research and Design*, *143*, 215–225.

Gao, H., & Stenstrom, M. K. (2019b). Evaluating the effects of inlet geometry on the flux capacity of secondary settling tanks with computational fluid dynamics model and one-dimensional flux theory model. *Journal of Environmental Engineering*, *145*, 04019065. https://doi.org/10.1061/(ASCE)EE.1943-7870.0001582

Gkesouli, A., Nitsa, M., Stamou, A., Rutschmann, P., & Bui, M. D. (2016). Modeling the effect of wind in rectangular settling tanks for water supply. *Desalination and Water Treatment*, *57*(54), 26345–26354.

Gkesouli, A., & Stamou, A. (2018). A CFD modeling procedure to assess the effect of wind in settling tanks. *Journal of Hydroinformatics*, *21*(1), 123–135.

Goodarzi, D., Lari, K. S., & Alighardashi, A. (2018). A large eddy simulation study to assess low-speed wind and baffle orientation effects in a water treatment sedimentation basin. *Water Science and Technology*, *2017*(2), 412–421.

Khezri, S. M., Biati, A., & Erfani, Z. (2012). Determination of the effect of wind velocity and direction changes on turbidity removal in rectangular sedimentation tanks. *Water Science and Technology*, *66*(12), 2814–2820.

Krebs, P., Stamou, A., Garcia-Heras, J. L., & Rodi, W. (1996). Influence of inlet and outlet configuration on the flow in secondary clarifiers. *Water Science and Technology*, *34*(5–6), 1–9.

Lakehal, D., Krebs, P., Krijgsman, J., & Rodi, W. (1999). Computing shear flow and sludge blanket in secondary clarifiers. *Journal of Hydraulic Engineering*, *125*(3), 253–262.

Larsen, P. (1977). *On the hydraulics of rectangular settling basins: Experimental and theoretical studies*. Department of Water Resources Engineering, Lund Institute of Technology, University of Lund.

McCorquodale, J. A., La Motta, E., Griborio, A., Georgiou, I., & Homes, J. (2004). *Development of software for modeling activated sludge clarifier system*. Technology Transfer Report Submitted to US EPA, Schielder Urban Environmental System Center, University of New Orleans, New Orleans, LA.

Parker, D. S. (1983). Assessment of secondary clarification design concepts. *Journal of Water Pollution Control Federation*, *55*(4), 349–359.

Patziger, M. (2016). Computational fluid dynamics investigation of shallow circular secondary settling tanks. Inlet geometry and performance indicators. *Chemical Engineering Research and Design*, *112*, 122–131.

Ramalingam, K., Xanthos, S., Gong, M., Fillos, J., Beckmann, K., Deur, A., & McCorquodale, J. A. (2012). Critical modeling parameters identified for 3D CFD modeling of rectangular final settling tanks for New York City wastewater treatment plants. *Water Science and Technology*, *65*(6), 1087–1094. https://doi.org/10.2166/wst.2012.944

Ramin, E., Wagner, D. S., Yde, L., Binning, P. J., Rasmussen, M. R., Mikkelsen, P. S., & Plosz, B. G. (2014). A new settling velocity model to describe secondary sedimentation. *Water Research*, *66*, 447–458.

Samstag, R. W., Dittmar, D. F., Vitasovic, Z., & McCorquodale, J. A. (1992). Underflow geometry in secondary sedimentation. *Water Environment Research*, *64*(3), 204–212.

Stamou, A., & Gkesouli, A. (2015). Modeling settling tanks for water treatment using computational fluid dynamics. *Journal of Hydroinformatics*, *17*(5), 745–762.

Takács, I., Patry, G. G., & Nolasco, D. (1991). A dynamic model of the clarification-thickening process. *Water Research*, *25*(10), 1263–1271.

Tecplot 360. Bellevue, Washington, USA. Retrieved from https://www.tecplot.com/products/tecplot-360/

Trelis 16.5. American Fork, Utah, USA. Retrieved from https://www.csimsoft.com

Vitasovic, Z. C., Zhou, S., McCorquodale, J. A., & Lingren, K. (1997). Secondary clarifier analysis using data from the Clarifier Research Technical Committee protocol. *Water Environment Research*, *69*(5), 999–1007.

Weiss, M., Plósz, B. G., Essemiani, K., & Meinhold, J. (2007). Suction-lift sludge removal and non-Newtonian flow behaviour in circular secondary clarifiers: Numerical modelling and measurements. *Chemical Engineering Journal*, *132*(1–3), 241–255.

Wicklein, E., & Samstag, R. W. (2009). *Comparing commercial and transport CFD models for secondary sedimentation*. In Proceedings of WEFTEC 09-82th Annual WEF Technical Exhibition and Conference, pp. 6066–6081. Orlando, FL.

Zhou, S., & McCorquodale, J. A. (1992a). Influence of skirt radius on performance of circular clarifier with density stratification. *International Journal for Numerical Methods in Fluids*, *14*(8), 919–934.

Zhou, S., & McCorquodale, J. A. (1992b). Mathematical modelling of a circular clarifier. *Canadian Journal of Civil Engineering*, *19*(3), 365–374.

Zhou, S., & McCorquodale, J. A. (1992c). Modeling of rectangular settling tanks. *Journal of Hydraulic Engineering Division of the American Society of Civil Engineers*, *118*(10), 1391–1405.